INTEGRATION OF PPP GPS AND LOW COST IMU

Shuang Du *, Yang Gao
Department of Geomatics Engineering, University of Calgary, 2500 University Dr NW, Calgary, Alberta, T2N1N4 Canada - (sdu, ygao)@ucalgary.ca

Commission I, Working Group I/5

KEY WORDS: PPP, MEMS IMU, Kalman filter, Loosely Coupled Integration, Tightly Coupled Integration

ABSTRACT:

GPS and low-cost INS integrated system are expected to become more widespread as a result of the availability of low cost inertial Micro-Electro-Mechanical Sensors (MEMS). Currently most of the integration systems are based on the differential GPS (DGPS) to ensure the navigation performance. However with the requirements of the base station, the system cost and complexity are significantly increased. With the advent of Precise Point Positioning (PPP), which is able to provide decimetre to centimetre accurate positioning accuracy without the need for a base receiver station, it opens the opportunity to develop a high performance GPS/INS navigation system based on only one GPS receiver. The motivation of this research is to investigate the integration of PPP GPS and low-cost INS such as MEMS for precise positioning and attitude determination. This paper will describe the PPP GPS technology and both loosely coupled and tightly coupled integration of PPP GPS and low-cost IMU. The navigation performance of integrated system of PPP GPS and low-cost IMU will be analyzed using road test dataset. The difference between loosely coupled system and tightly coupled system will also be analyzed based on the numerical results.

1. INTRODUCTION

Nowadays GPS and low cost INS integrated system are expected to become more widespread as a result of the availability of low cost inertial Micro-Electro-Mechanical Sensors (MEMS). The integration of GPS and INS has been a hot research area over the past decades and successfully applied in many applications such as vehicle navigation, direct geo-referencing of aircraft. Hide and Moore (2005) investigated the GPS and low cost INS integration for positioning in the urban environments. Godha (2006) investigated the obtainable performance of the integrated DGPS and low cost MEMS IMU. Edwan et al, (2009) developed a constrained GPS/INS integration based on rotation angle for attitude update and dynamic model for position update. Research and investigations were also conducted to incorporate the GPS/INS system with other sensors, such as magnetometer, odometer or multiple GPS antenna. Hirokawa et al (2008) integrated the low cost GPS/INS system with a GPS compass. Tao (2009) investigated the GPS/Reduced MEMS IMU with a wheel speed sensor to improve the obtainable navigation performance.

Currently most of the integration systems and research are based on the differential GPS (DGPS) to ensure the navigation performance. However the requirement on base station is usually problematic as it limits the operational range of the system and also increases the system cost and complexity. With the advent of Precise Point Positioning (PPP), which is able to provide decimetre to centimetre accurate positioning accuracy without the need for a base receiver station, it opens the opportunity to develop a high performance GPS/INS navigation system based on only one GPS receiver. Previous work has demonstrated that the integration of PPP and tactical grade IMU is able to provide high quality position and velocity solution with accuracy of decimetre to sub-decimetre for position and centimetre per second for velocity (Zhang and Gao, 2007). However, due to the expensive cost of a tactical grade IMU, it is applicable only to limited applications.

The motivation of this research is to investigate the obtainable performance of an integrated system based on precise point positioning GPS and low cost MEMS IMU. This paper will describe the PPP GPS technology and both loosely coupled and tightly coupled integration of PPP GPS and low-cost IMU. The navigation performance of an integrated PPP GPS and low-cost IMU system will be analyzed using road test dataset. The difference between loosely coupled system and tightly coupled system will also be analyzed based on the numerical results.

This paper is organized as follows. Section 2 introduces the precise point positioning GPS and Section 3 describes the integration of PPP GPS and low cost MEMS IMU, including both loose integration and tight integration. Section 4 presents the conducted field test, the numerical results and analysis. The conclusions and future work are given in Section 5.

2. PRECISE POINT POSITIONING

Precise Point Positioning is a positioning methodology, using un-differenced GPS phase and code measurements from a single dual frequency receiver and the precise orbit and clock product generated by service providers such as International GNSS Service (IGS). The proper use of the carrier phase observations as the primary observable can lead to decimetre and sub-decimetre accuracy of point positioning (Kouba and Heroux, 2000).

2.1 Error Sources and Mitigation Technique in PPP

The GPS errors include satellite orbit and clock offset, atmosphere error, multipath and noise. Unlike DGPS, those

* Corresponding author.

errors cannot be eliminated by differencing algorithm between receivers since no location base stations are available in PPP. The satellite orbit and clock error are eliminated by applying the precise GPS orbit and clock products. The IGS provides precise GPS orbit and clock products at different latencies and accuracies and more details can be found at: http://igscb.jpl.nasa.gov/components/prods.html.

The slant tropospheric delay contains two components, the hydrostatic and wet delays. Each of them can be represented by a zenith delay and a mapping function. The hydrostatic delay contains 90% of the total tropospheric delay and its modeling can achieve millimetre accuracy (Aldel-Salam, 2005). The tropospheric wet delay will be estimated in PPP along with other parameters of interest. With dual-frequency observations, the first order ionospheric delay can be eliminated by forming ionosphere-free combinations. More details will be provided in Section 2.2.

Receiver clock offset is estimated along with other parameters of interest, while rest errors such as satellite antenna offsets, phase wind up correction, earth tide effect will be mitigated by modeling.

2.2 PPP Observation Model

Two observation models, known as the traditional model and the UofC model, are often used in PPP. The traditional model consists of the ionosphere-free code and carrier phase observation combinations as illustrated in equation (1) (Aldel-Salam, 2005):

$$
\begin{aligned}
P_{IF} &= \frac{f_1^2 P_1 - f_2^2 P_2}{f_1^2 - f_2^2} = \rho + c \cdot dT + m(e) d_w + dm_{IF} + \varepsilon(P_{IF}) \\
\Phi_{IF} &= \frac{f_1^2 \Phi_1 - f_2^2 \Phi_2}{f_1^2 - f_2^2} = \rho + c \cdot dT + m(e) d_w \\
&+ \frac{c \cdot f_1 \cdot N_1 - c \cdot f_2 \cdot N_2}{f_1^2 - f_2^2} + dm_{IF} + \varepsilon(P_{IF})
\end{aligned}
\tag{1}
$$

where f_1 and f_2 are the L1 and L2 frequency, P_1 and P_2 are GPS code measurements on L1 and L2 frequency, Φ_1 and Φ_2 are GPS phase measurements on L1 and L2 frequency, dT is the receiver clock error, d_w is wet component of the tropospheric delay, dm_{IF} is the multipath, ε is the noise, m(.) is the mapping function, e represents the elevation angle. The traditional model allows for the estimation of the ionosphere-free ambiguities, the receiver clock offset, and the wet component of the tropospheric delay. The ambiguities will be estimated as float values.

The UofC model uses an average of code and carrier phase observation on L1 and L2 in addition to the ionosphere-free carrier phase combination. The average of code and carrier phase observation is used to eliminate the first-order ionospheric delay. More details are presented at Abdel-Salam (2005).

3. INTEGRATION OF PPP AND MEMS IMU

In general, the loose and tight integration strategies are the most common used at the user-level. They differ only in the type of information shared between GPS and INS (Petovello, 2003). The details of a loose integration and a tight integration of PPP and low cost MEME IMU are described in the following sections.

3.1 Loose Integration

In loose integration, the PPP and inertial processing is carried out in two separate, but interacting filters, namely PPP filter and integration filter. The integration strategy is illustrated in Figure 1.

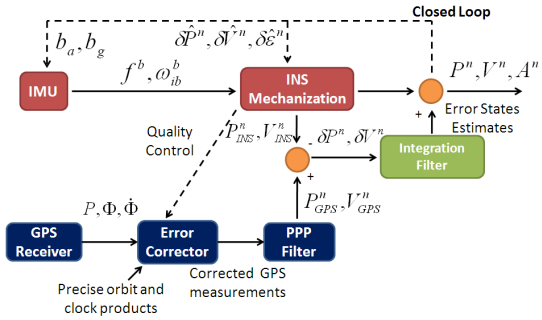

Figure 1. PPP/MEMS IMU loose integration scheme

The integrated system contains 3 components, namely the INS component, the PPP component and the integration filter component. The integration filter uses the difference between the PPP-derived positions and velocities and the INS mechanization-derived positions and velocities as measurements to compute the error estimates. The error corrector in the PPP component is used to correct the errors in the raw GPS measurements, with more details in Section 2. The closed loop approach is used to feed these error states to the INS component to correct the INS errors. The output of the INS mechanization could also be applied in PPP error corrector to help the quality control of the integrated system, such as cycle slip detection and identification.

The loose integration strategy is very common due to its simplicity of implementation and robustness. However, the primary disadvantage of this strategy is that the integrated system provides poor solution during periods of partial GPS availability (typically less than 4 satellites) and the tight integration strategy will outperform this strategy under such situations. Petovello (2003) identifies one specific problem with loose integration that the processing noise has to be added to both of the filters because the system has two independent filters. The extra processing noise in the GPS filter used to compensate the user's dynamics would have also negative effect on the state estimation.

Integration Filter States

MEMS IMU, such as Crista IMU, normally features a turn-on bias of about 5400 deg/h in gyros, while these biases are negligible in higher grade IMUs. Also, the MEMS IMU exhibits in-run bias drift of more than 1000 deg/h, compared to 1 deg/h for a tactical grade IMU (Godha, 2006). Since it is not practical to calibrate them each time when the sensor is turned on, a solution is to estimate these errors as additional states in

Kalman filter. By considering the position errors, velocity errors, attitude errors, and the additional sensor bias drifts, turn on biases and scale factor errors for low cost MEMS IMU, a 27-error states vector is formed as equation (2).

$$x_{INS} = [\delta r^l, \delta v^l, \delta \varepsilon^l, \delta b_a, \delta b_g, b_{a,tob}, b_{g,tob}, S_a, S_g] \quad (2)$$

where $\delta r^l = [\delta\varphi \quad \delta\lambda \quad \delta h]$ is the position error state vector in l-frame, $\delta v^l = [\delta v_E \quad \delta v_N \quad \delta v_U]$ is the velocity error state in l-frame, $\delta\varepsilon^l = [\delta\theta \quad \delta\phi \quad \delta\psi]$ is the attitude error state vector, S_i is the scale factor error, $b_{i,tob}$ is the sensor turn on the bias and δb_i is the bias drift (δb_i).

Integration Filter Mathematical Model

The INS error model can be derived from the perturbations of the INS mechanization equations as described by equation (3) (Jekeli, 2001).

$$\begin{aligned}
\delta\dot{r}^l &= F_{rr}\delta r^l + F_{rv}\delta v^l \\
\delta\dot{v}^l &= F_{vr}\delta r^l + F_{vv}\delta v^l + F_{v\varepsilon}\delta\varepsilon^l + R_b^l\delta b_a + R_b^l b_{a,tob} + R_b^l f^b S_a \\
\delta\dot{\varepsilon}^l &= F_{\varepsilon r}\delta r^l + F_{\varepsilon v}\delta v^l + F_{\varepsilon\varepsilon}\delta\varepsilon^l + R_b^l\delta b_g + R_b^l b_{g,tob} + R_b^l\Omega_{ib}^b S_g
\end{aligned} \quad (3)$$

where $F_{rr}, F_{rv}, F_{vr}, F_{vv}, F_{v\varepsilon}, F_{\varepsilon r}, F_{\varepsilon v}, F_{\varepsilon\varepsilon}$ are the relationship matrix among the position error states, velocity error states and attitude error states. The details of the above matrix and the full derivation of error equations are presented at Jekeli (2001).

The sensor bias-drift and scale factor errors are modelled as a first order Gauss Markov process, and the turn on bias is modelled as a random constant process in the filter since it remains constant after the sensor is turned on.

Integration Filter Measurement Model

The measurement model is the same as the usually used measurement model of loosely coupled integrated GPS/INS system. The measurement noise of the integration filter is generated by transferring the full position and velocity variance covariance matrix from the PPP filter to ensure that the correlation between the PPP processed position and velocities are properly accounted.

3.2 Tight Integration

In a tight integration scheme, a single integration filter is used to fuse the GPS and INS information, as illustrated in Figure 2. Different from the loose integration, the outputs of the INS mechanization are not directly used in the integration filter, instead it is used to predict the GPS measurements, such as the pseudorange, the carrier phase and the Doppler measurements. Later, the PPP corrected pseudorange, carrier phase and Doppler measurements are differenced with the INS predicted measurements. The integration filter directly processes those residuals to obtain the INS error estimates. Finally the obtained error estimates are feed back to the INS component by using the closed loop approach.

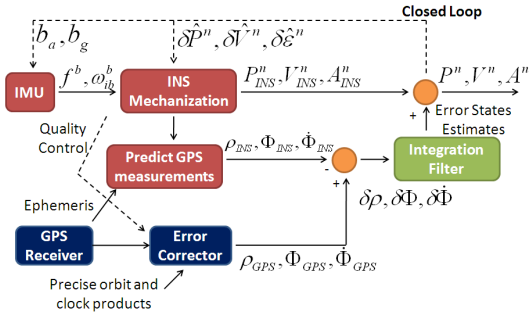

Figure 2. PPP/MEMS IMU tight integration scheme

A tight integration strategy is preferred to use in urban canyons, which is a situation in which the number of the tracked satellites is frequently less than 4, because the INS can still be updated with available GPS pseudorange, carrier phase or Doppler measurements. In addition, because no additional processing noise is present in the single filter and the GPS measurements used to update the filter are more statistically independent than the position and velocity states, this strategy offers better accuracy on the estimated states. However compared to the loosely coupled strategy, the increased size of the state vector leads to an increased computational burden (Petovello, 2003; Tao, 2009).

Integration Filter States

Since there is only one filter to process both GPS and INS information in a tight integration, the filter must account for not only the INS error states but also the PPP states, such as the receiver clock error state, the wet component of the tropospheric delay and the ambiguity terms. The full filter state vector can be described by equation (4).

$$x = [x_{INS}, dT, d_{dT}, d_w, N_{IF,1}, N_{IF,2} \cdots N_{IF,i}] \quad (4)$$

where dT and d_{dT} are the receiver clock error and receiver clock error rate, respectively; d_w is the wet component of tropospheric delay, and $N_{IF,i}$ is the ionosphere-free ambiguity for ith satellite.

Integration Filter Mathematical Model

For the original 27 INS error states, the error model remains the same as in loose integration; while for the additional PPP states, the mathematical model can be described as equation (5).

$$\begin{bmatrix} \dot{dT} \\ \dot{d}_{dT} \\ \dot{d}_w \\ \dot{N}_{IF,i} \end{bmatrix} = \begin{bmatrix} 0 & 1 & 0 & 0 \\ 0 & 0 & 0 & 0 \\ 0 & 0 & 0 & 0 \\ 0 & 0 & 0 & 0 \end{bmatrix} \begin{bmatrix} dT \\ d_{dT} \\ d_w \\ N_{IF,i} \end{bmatrix} + \eta \quad (5)$$

where η is the system noise.

Integration Filter Measurement Model

The integration filter processes the residuals between the GPS pseudorange, carrier phase and Doppler measurements and the corresponding INS predicted pseudorange, carrier phase and Doppler measurements to estimate the error states. Thus, the measurement design matrix and misclosure vector can be written as equation (6) and equation (7) (Zhang and Gao, 2007).

$$H = \begin{bmatrix} A_j & 0 & 0 & 0 & 0 & 0 & 0 & -c & 0 & m(e)_w & 0 & \\ A_j & 0 & 0 & 0 & 0 & 0 & 0 & -c & 0 & m(e)_w & 0 & \cdots \\ B_j & C_j & 0 & 0 & 0 & 0 & 0 & 0 & -c & 0 & \lambda_{IF} & \cdots \\ & & & & & \vdots & \vdots & & & & & \end{bmatrix} \quad (6)$$

$$Z = \begin{bmatrix} P_j^{GPS} - P_j^{INS} \\ \Phi_j^{GPS} - \Phi_j^{INS} \\ \dot{\Phi}_j^{GPS} - \dot{\Phi}_j^{INS} \\ \vdots \end{bmatrix} \quad (7)$$

where $P_j^{GPS} - P_j^{INS}, \Phi_j^{GPS} - \Phi_j^{INS}, \dot{\Phi}_j^{GPS} - \dot{\Phi}_j^{INS}$ are the residuals between the PPP corrected ionosphere-free pseudorange, carrier phase and phase rate, and INS predicted pseudorange, carrier phase and phase rate from the GPS receiver to the j-th satellite, respectively, $A_j = \frac{\partial P_j}{\partial \gamma}, B_j = \frac{\partial \dot{\Phi}_j}{\partial \gamma}$ and $C_j = \frac{\partial \dot{\Phi}_j}{\partial V}$ are the partial derivatives of the range, phase and phase rate with respect to the receiver position and velocity.

3.3 Non Holonomic Constraints

The non-holonomic constraints are commonly used to maintain or improve the navigation performance. The constraints used in this paper are 2D velocity constraints which are derived based two assumptions. The first assumption is that the vehicle does not slip, which is a close representation for vehicle travelling in a constant direction. The second assumption is that the vehicle stays on the ground. If both the assumptions are true, then the velocity of the vehicle in the direction perpendicular to the movement of the vehicle can be regarded as zero (Godha, 2006; Tao, 2009).

The measurement model for the 2D velocity constraints can be obtained by a perturbation of the b-frame velocity as illustrated in equation (8) (Tao, 2009).

$$Z = R_l^b \delta v^l + \begin{bmatrix} 0 & -v_z^b & v_y^b \\ v_z^b & 0 & -v_x^b \\ -v_y^b & v_x^b & 0 \end{bmatrix} \begin{bmatrix} \delta\theta \\ \delta\phi \\ \delta\psi \end{bmatrix} + \eta \quad (8)$$

η represents the measurement noise of the 2D velocity constraints, and it is calculated based on a projection of the forward velocity on the lateral and up direction due to the misalignment angles (Godha, 2006; Tao, 2009). The typical forward velocity of a land vehicle is 18~20 m/s in most cases, and if the misalignment is 2~3 degrees the projected velocity on the lateral direction and up direction is around 1 m/s. Thus, normally the measurement noise can be set to 1 m/s.

4. FIELD TEST AND RESULTS ANALYSIS

4.1 Field Test Description

The field test was conducted at the residential areas in Calgary, Alberta. The equipments used are SPAN^{TM} system and NavBox. The SPAN^{TM} system consists of a NovAtel OEM4 receiver and an HG1700AG11 IMU (HG1700), which is a tactical grade IMU. The NavBox was developed by the PLAN group at the University of Calgary. It consists of a NovAtel receiver and a Crista IMU. The raw dual frequency GPS pseudorange, carrier phase and Doppler measurement were logged from the SPAN^{TM} system with a data rate of 1 Hz and the raw IMU data from HG1700 was logged at a rate of 100 Hz. The Crista IMU data was also collected at 100 Hz, and it was synchronized by the NovAtel GPS receiver inside the NavBox. In order to generate a reference solution using a high precision DGPS/INS integrated system, a NovAtel OEM4 receiver was setup on a building roof at The University of Calgary to act as the base station. The raw GPS pseudorange, carrier phase and Doppler measurements in dual-frequency were logged at 1 Hz for the base station. The duration of the field test was conducted for about 20 minutes.

In order to evaluate the navigation performance of the proposed integrated PPP/MEMS system, a reference navigation solution is generated by using the loosely coupled DGPS and HG1700 data. The DGPS solution was obtained by using the Waypoint GrafNav 8.10 software. The dual frequency GPS carrier phase, pseudorange, and Doppler measurements are all used in the processing. The noise parameter of HG1700 can be found in Petovello (2003). The reference solution is accurate to better than 5 centimetres for position, while the attitude solution is accurate at 0.03 degree for the pitch and roll, and 0.17 degree for the azimuth (Godha, 2006).

4.2 PPP-only Solution

In order to assess the performance of the integrated system, it is necessary to examine the performance of the aiding source, which is the PPP. The satellites visibility and PDOP are shown in Figure 3. The figure indicates that the satellite visibility and geometry are relatively poor at some epochs. Since the GPS data were collected at the residential area, the RF signal is frequently blocked by houses or trees, which leads to a relatively poor satellite geometry.

Table 1 presents a statistical summary of the PPP only solution accuracy. Since the duration of the GPS data is less than 20 minutes, the ambiguity of carrier phase cannot be completely converged; the backward processing method is employed to improve the obtainable accuracy. As it can be seen, the root mean square (RMS) errors are 0.10 m, 0.32 m and 0.47 m for latitude, longitude and height, respectively. The velocity errors are around 2 cm/s for the horizontal and 8 cm/s for vertical component. The obtainable accuracy for PPP only solution is decimetre level for position, and centimetre to sub decimetre per second level for velocity. Since the obtainable accuracy of the GPS/INS integrated system depends on the accuracy of the GPS solution, a similar accuracy level is expected from the integrated solution.

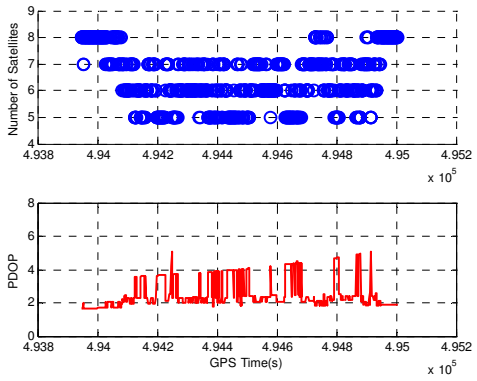

Figure 3. Number of satellites and PDOP

Unit: m	Lat	Lon	Height
RMS	0.10	0.32	0.47
Unit: m/s	Ve	Vn	Vu
RMS	0.019	0.025	0.076

Table 1. Statistical summary of PPP-only solution accuracy

4.3 Tightly Coupled PPP/Crista Solution

Figure 4 shows the position errors and velocity errors in tightly coupled system. Since more than four GPS satellites were available throughout the entire run, it prevents the INS error accumulation. Table 2 presents a statistical summary of the position and velocity errors. Improvements are observed at the integrated system solution. The results indicated that the tightly coupled PPP/Crista system offers decimetre level position accuracy and centimetre to sub-decimetre per second level velocity accuracy.

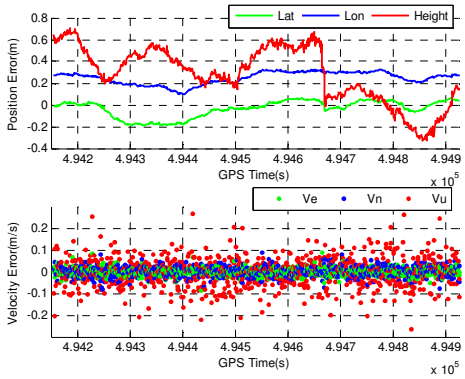

Figure 4. Position error and velocity error in tightly coupled solution

Figure 5 shows the attitude errors. Due to the large sensor errors and poor observability, especially when absence of horizontal accelerations, the azimuth errors are relative large compared to the tactical grade IMU. Table 2 shows a statistical summary of the attitude errors. Comparing those numbers with the typical DGPS/MEMS attitude accuracy, for instance, and without applying any non-holonomic constraints, the pitch errors and roll errors are 0.3~0.5 degree, and azimuth errors are 1.2~1.6 degrees (Godha, 2006; Tao, 2009), the tightly coupled PPP/MEMS integrated system offers promising results which use only a single GPS dual-frequency receiver.

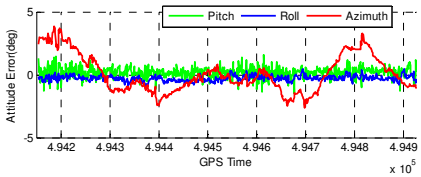

Figure 5. Attitude error in tightly coupled solution

It has been found that the non-holonomic constraints are able to improve the attitude accuracy (Tao, 2009). Figure 6 shows the attitude error after applying the derived 2D velocity constraints, and Table 2 shows the statistical summary. Improvements are found on all attitude states, especially for azimuth. The RMS value of the azimuth errors has been improved from 1.41 degrees to 0.75 degree.

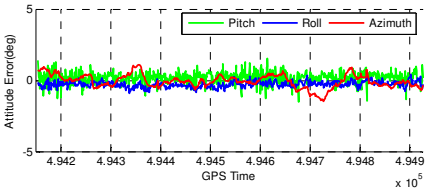

Figure 6. Attitude error in tightly coupled solution after applying 2D velocity constraints

Unit: m	Lat	Lon	Height
RMS	0.08	0.26	0.38
Unit: m/s	Ve	Vn	Vu
RMS	0.018	0.023	0.072
Unit: degree	Pitch	Roll	Azimuth
RMS	0.44	0.37	1.41
2D Constraints	0.42	0.35	0.75

Table 2. Statistical summary of tightly coupled solution

As indicated in equation (8), the lateral velocity error is related to velocity error in the local level frame, the roll error state and azimuth error state through the transformation matrix from the b-frame to the l-frame, the vertical velocity in the b-frame and the forward velocity in the b-frame, respectively. Since the velocity error states are directly observed in the integration filter, the contribution of the lateral velocity constraint is mainly on the roll estimate and azimuth estimate. Normally, the forward velocity is much larger than the vertical velocity, so the azimuth estimate accuracy is significantly improved when compared to the roll estimate.

Similarly, the vertical velocity error is related to the velocity error states in the l-frame, the pitch error and roll error states. So the improvement is also expected to be seen on both roll and pitch estimate, which has been confirmed by results shown in Table 2.

Both the azimuth error state and pitch error state are related to the 2D velocity constraints through the forward velocity in the b-frame. However the vertical velocity constraint only has a minor effect on the pitch estimate compared to the lateral velocity constraint which has a major effect on the azimuth. The reason is twofold. First the pitch estimate has a better observability, which leads to a better estimate, since it does not rely on the presence of the horizontal acceleration but the vertical acceleration. Second, the measurement noise level of

the vertical velocity measurements are set to relatively large to make sure it will not has a negative effect on the navigation performance.

4.4 Loosely Coupled PPP/Crista Solution

Table 3 shows a statistical summary of the resulting position, velocity and attitude errors in loosely coupled system. Similar to the tightly coupled solution, GPS availability prevents the INS error accumulations, which results in a decimetre level accuracy for position, and centimetre to sub-decimetre per second for velocity. The loosely coupled system offers similar attitude solution compared with the tightly coupled system. The RMS attitude errors are better than 0.5 degree for both roll and pitch, and 1.42 degrees for azimuth. After applying the 2D velocity constraints, improvements are observed on all attitude states, especially for azimuth. The RMS value of the azimuth error is improved from 1.42 degrees to 0.80 degree.

It can be seen that both the tightly coupled and loosely coupled PPP/MEMS system is able to offer high quality solution, which is comparable to a DGPS/MEMS system. The tightly coupled system offers slightly better results than the loosely coupled system. This is because GPS and INS information are more rigorously modeled in the tight integration than a loosely coupled system

Unit: m	Lat	Lon	Height
RMS	0.10	0.30	0.40
Unit: m/s	Ve	Vn	Vu
RMS	0.019	0.025	0.073
Unit: degree	Pitch	Roll	Azimuth
RMS	0.46	0.43	1.42
2D Constraints	0.43	0.41	0.80

Table 3. Statistical summary of loosely coupled solution

5. CONCLUSIONS AND FUTURE WORK

This paper investigates the obtainable accuracy of an integrated GPS/INS system based the precise point positioning GPS and low cost MEMS IMU. In both loose and tight integrations, GPS measurements from a dual frequency GPS receiver, such as pseudorange, carrier phase and Doppler measurements are used. Based on obtained numerical results, the integrated PPP/MEMS IMU system is able to offer high quality navigation solution with decimetre level accuracy for position, and centimetre to sub-decimetre per second level accuracy for velocity.

The integrated PPP and low cost MEMS IMU system offers better than 0.5 degree for both pitch and roll, and better than 1.5 degrees for azimuth, which is similar to the attitude accuracy of integrated DGPS and low cost MEMS IMU system using dual GPS receivers (one of them serves as the base station), for instance, 0.3~0.5 degree for pitch and roll and 1.2~1.6 degrees for azimuth (Godha, 2006; Tao, 2009). By applying the derived 2D velocity constraints, the attitude accuracy can be further improved, especially for the azimuth estimate. The RMS value of the azimuth errors can be reduced from 1.4 degrees to about 0.8 degree.

The future work will include the investigation of the obtainable accuracy of the proposed system using only pseudorange or single frequency data, and during GPS partial outages, especially under hostile environments, such as urban canyon environments.

References

Abdel-Salam, M., 2005. Precise Point Positioning Using Un-Differenced Code and Carrier Phase Observations. Ph.D. Dissertation. Department of Geomatics Engineering, The University of Calgary.

Edwan, E., Knedlik, S., Zhou, J., and Loffeld, O., 2009. A constrained GPS/INS Integration Based on Rotation Angle for Attitude Update and Dynamic Models for Position Update. Proceedings of ION 2009 International Technical Meeting, Anaheim, CA, January 26-28, 2009.

Godha, S., 2006. Performance Evaluation of Low Cost MEMS-Based IMU Integrated With GPS for Land Vehicle Navigation Application. MSc Thesis. Department of Geomatics Engineering, The University of Calgary.

Hide, C. and Moore, T., 2005. GPS and Low cost INS Integration for Positioning in Urban Environment. Proceedings of ION GNSS 2005, Long Beach, CA, September 2005.

Hirokawa, R., Kajiwara, N., Ohata, R., and Suzuki, T., 2008. Performance Evaluation of Low Cost Multi-Antenna GPS/INS for Small UAVs. Proceedings of ION GNSS 2008, Savannah, GA, USA, September 2008.

Jekeli, C., 2001. *Inertial Navigation Systems with Geodetic Applications*. Walter de Gruyter, pp.101-134.

Kouba, J. and Heroux, P., 2000. Precise Point Positioning Using IGS Orbit and Clock Products. *GPS solutions*, Volume 5, No 2, October, 2001, Springer Berlin Publications, pp. 12-28.

Petovello, M., 2003. Real-Time Integration of a Tactical-Grade IMU and GPS for High-Accuracy Position and Navigation. Ph.D. Dissertation, Department of Geomatics Engineering , University of Calgary, Canada.

Tao, L., 2009. Use of Wheel Speed Sensors to Enhance a Reduced IMU Ultra-Tight GNSS Receiver. MSc Thesis. Department of Geomatics Engineering, The University of Calgary,

Zhang, Y. and Gao, Y., 2007. Integration of INS and Un-differenced GPS Measurements for Precise Position and Attitude Determination. *The Journal of Navigation*, 61, The Royal Institute of Navigation, pp.1-11.

Acknowledgement

The field test data provided by PLAN group at The University of Calgary is greatly acknowledged.